

Ultra-compact Half-Mode SIW FPDs with Arbitrary Power Division Ratios Using Spiral Technique

- M. Danaeian*** [Corresponding Author] Electrical Eng. Dept.; Vali-e-Asr University of Rafsanjan; Rafsanjan, Iran Email: danaeian@vru.ac.ir
- MM. Pezhman** Electrical Eng. Dept.; Graduate university of advanced technology; Kerman, Iran Email: pezhmanmehdi@ymail.com
- H. Baniasadi** Electrical Eng. Dept.; Vali-e-Asr University of Rafsanjan; Rafsanjan, Iran; Email: hbeniasadi@gmail.com
- H. Noori** Electrical Eng. Dept.; Vali-e-Asr University of Rafsanjan; Rafsanjan, Iran; Email: h.noori@vru.ac.ir

Received: 07 Dec. 2021

Revised: 12 Apr. 2022

Accepted: 28 Apr. 2022

Abstract: Three ultra-compact half-mode substrate integrated waveguide (HMSIW) equal/unequal filtering power dividers (FPDs) based on the metamaterial concept and the evanescent mode technique are recommended in this paper. The spiral technique is a well-known technique in planar microwave circuitry. By combining the spiral technique and the conventional complementary split-ring resonator (CSRR) unit cell, the complementary spiral resonator (CSR) unit cell can be achieved. The resonance frequency of the two-turns CSR unit cell is half the resonance frequency of the conventional CSRR unit cell with the same size and shape. Accordingly, the electrical size of the CSR unit cell is smaller than the conventional CSRR unit cell with the same physical size. According to the evanescent technique, by loading the CSR unit cell on the metal surface of the HMSIW structure, an extra forward passband can be obtained. Therefore, three miniaturized equal/unequal FPDs with arbitrary power-dividing ratios of 1:1, 1:4, and 1:8 have been designed, simulated, fabricated and measured based on the compact HMSIW-CSR structure. A reasonable agreement between simulated and measured results has been achieved. The fractional 3-dB bandwidth of the designed equal/unequal FPDs are approximately 21 % at 2.4 GHz. The whole dimension of the proposed FPDs is about $0.06 \lambda_g \times 0.06 \lambda_g$ which confirms the small size of the presented structures.

Index Terms: Half-mode Substrate Integrated Waveguide (HMSIW), Filtering Power Divider (FPD), Complementary Spiral Resonator (CSR), Evanescent Mode Technique, Miniaturization.

Citation: M. Danaeian, MM. Pezhman, H. Baniasadi and H. Noori, "Ultra-compact Half-Mode SIW FPDs with Arbitrary Power Division Ratios Using Spiral Technique," *Journal of Communication Engineering*, vol. 11, no. 1, pp. 21-40, Jan.-Jun. 2024.

 <http://dx.doi.org/10.22070/jce.2024.18694.1264>

I. INTRODUCTION

The filtering power divider (FPD) is a dual-functional module in modern wireless communication systems which is realized by combining the bandpass filter (BPF) component and power divider (PD) component into one component [1–17]. The FPD with arbitrary output power division ratios is widely used in the feeding network in antenna applications that can reduce the insertion loss and side-lobe levels. Several FPDs have been recently studied [1-17]. A miniaturized equal/unequal SIW power divider with bandpass filtering response loaded by complementary split-ring resonators (CSRRs) is proposed in [1]. In [2], A miniaturized SIW power divider with embedded filter response and arbitrary power dividing ratio loaded by open complementary split-ring resonators (OCSRRs) is presented. In [3], two ultra-compact power dividers based on the SIW and half-mode SIW (HMSIW) technologies loaded by CSRRs are presented. In [4], a four-way FPD based on a SIW using two layers of the dielectric substrate and based on the eighth-mode SIW (EMSIW) technique is developed. In [5], a compact single-layer FPD based on third-mode circular SIW cavities is introduced. Three miniaturized equal/unequal FPDs using the stepped-impedance resonator (SIR) technique applying the HMSIW and metamaterial concepts are offered in [6]. A novel ultra-compact fractal/meander CSRR (FMCSRR) HMSIW FPDs using metamaterial unit-cell based on the fractal technique and meander technique is introduced in [7]. In [8], a FPD based on air-filled SIW (AFSIW) technology for substantially reducing the transmission losses is proposed. Additionally, [9] introduces butterfly-shaped spoof surface plasmon polaritons (SSPPs) to design a broadband bandpass filter and FPD with enhanced slow-wave effect, compact size, and wide stopband. A packaged FPD with low radiation loss and low electromagnetic interference is investigated and synthesized in [10]. A class of multiway wideband FPDs using three-line coupled lines with a wide isolation band is designed in [11]. In [12], new class of wideband unequal power divider with enhanced power dividing ratio, fully matching bandwidth, and filtering performance is presented. A new concept for the in-phase power divider is presented based on four-port common-mode network (CMN) is presented in [13]. In [14], a wideband FPD using vertically installed planar (VIP) circuit is proposed. In [15], a microstrip high selectivity FPD with coupling from source/load to the resonator utilizing the pairs of parallel-coupled lines and asymmetrical T-shaped resonators is designed. A FPD based on a novel tri-mode resonator (TMR) is proposed in [16]. A four-way out-of-phase wideband FPD by using a multiport out-of-phase topology, and a pair of multimode U-shape slotline resonators is introduced in [17]. Although these presented structures have good performance, however, some of these implementations did not provide a filtering response and suffer from high insertion loss, low selectivity, high fabrication cost,

large size and high complexity of the manufacturing process [1-17].

The substrate-integrated waveguide (SIW) structure provides a new way to implement the traditional three-dimensional metallic waveguides in a planar form. The SIW structure has unique benefits in terms of high power handling capability, and easy integration with other passive components [1-9]. But still, the devices implemented with the SIW structures have large dimensions compared to the microstrip structures. The half-mode SIW (HMSIW) technique, is a miniaturization technique that halves the size of the SIW structures without disrupting the performance and efficiency of the SIW structures [1-9].

To further reduce the size of the devices and circuits realized by the HMSIW structure, using the concept of metamaterial can be useful. The complementary split ring resonator (CSRR) is considered as electric dipoles when excited by an axial electric field that exhibits negative permittivity in planar technologies [1-7]. Therefore, the CSRR unit cell is a good candidate for the design of negative effective permittivity and left-handed media in a limited frequency range. For higher levels of miniaturization, the spiral technique has been used to design the novel CSRR unit cell. The conventional CSRR unit cell is formed by two coupled aperture rings printed on a dielectric slab, while the two turns complementary spiral resonator (CSR) is made by a single aperture rolled up to form a spiral [18]. The electrical size of a two-turn CSR unit cell is roughly half the electrical size of the conventional CSRR unit cell, provided dimensions are identical. Obviously, by increasing the number of turns of the spirals, it is possible to further decrease their electrical size.

In this study, three ultra-compact equal/unequal FPDs using the HMSIW structure loaded by the CSR unit cell are proposed. The evanescent mode technique, the half-mode technique, and the spiral technique have been employed, simultaneously to miniaturize the total dimension of the proposed equal/unequal FPDs. The working principle of the proposed FPDs is based on the evanescent-mode technique. According to this technique, an extra passband below the waveguide cutoff frequency can be achieved by loading the electric dipoles on the metal cover of the HMSIW structure. Consequently, by a combination of the CSR unit cell and HMSIW structure, a forward transmission band has been achieved. Three samples of the proposed FPDs with different power division ratios of 1:1, 1:4, and 1:8 have been fabricated and measured. The measurements agree very well with the simulations. The proposed FPDs have many benefits such as very compact size, low cost, low loss, high selectivity, high power-handling capability, and easy integration with planar circuits.

II. Design of the Complementary Spiral Resonator (CSR) Configuration

The conventional complementary split-ring resonator (CSRR) unit cell is a well-known resonant metamaterial particle that provides a strong electric dipole in the vicinity of its resonant frequency and exhibits negative permittivity. As is well known, the complementary of a planar metallic structure is obtained by replacing the metal parts of the original structure with apertures, and the apertures with metal plates. The spiral technique is a valuable technique in planar microwave circuitry. By combining the spiral technique and the conventional complementary split-ring resonator (CSRR) unit cell, the complementary spiral resonator (CSR) unit cell can be achieved. The conventional CSRR unit cell is formed by two coupled aperture rings printed on a dielectric slab, while the two turns complementary spiral resonator (CSR) is made by a single aperture rolled up to form a spiral [18]. Similarly, the CSR unit cell acts as electric dipoles when excited by an axial external electric field, and an ϵ -negative can be obtained in a narrow band near its resonant frequency. The resonance frequency of the two-turns CSR unit cell is half the resonance frequency of the conventional CSRR unit cell with the same size and shape. Consequently, the electrical size of a two-turn CSR unit cell is roughly half the electrical size of the conventional CSRR unit cell, provided dimensions are identical. Obviously, the electrical size can still be reduced by increasing the number of turns of the spirals. Fig. 1 shows the conventional CSRR unit cell and the proposed CSR unit cell with the same sizes, respectively. The CSR unit cell can be modeled as a parallel resonant tank with inductance L_r and capacitance C_r . The C_r is the capacitance of a rectangular-shaped plate surrounded by a metallic plane, and L_r is the inductance of the metallic strip between the ring slots. Therefore, the resonance frequency of the CSR unit cell is calculated from [1-7]:

$$f_r = \frac{1}{2\pi\sqrt{L_r C_r}} \quad (1)$$

The spiral slot line on the CSR unit cell causes higher inductance and capacitance. Consequently, the resonance frequency of the CSR unit cell is decreased compared to the conventional CSRR with the identical sizes. This means that the electrical size of the CSR is decreased without occupying the extra space and miniaturization has been occurred. Therefore, a downward frequency shift in the frequency responses of the proposed CSR structure compared to the conventional CSRR structure is obtained. The results show that miniaturization of about 50% is achieved.

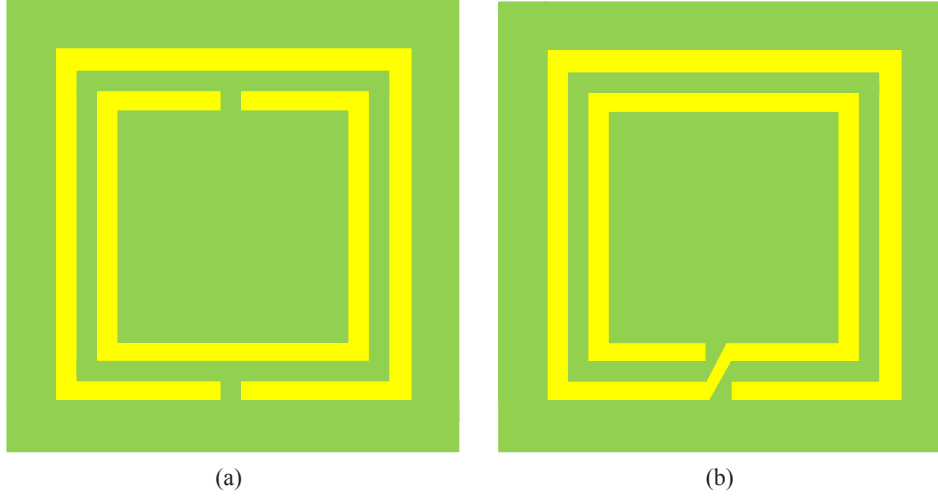


Fig. 1. Configuration of the (a) conventional CSRR unit cell, and (b) CSR unit cell

III. Design Procedure of the Proposed HMSIW-CSR FPDs

The substrate-integrated waveguide (SIW) structure provides a new way to implement the traditional three-dimensional metallic waveguides in a planar form. In the SIW structure, two metal plates on the top and bottom sides of the substrate are connected by two rows of metalized via holes which are used to form the electric sidewalls of the waveguide. The top metal layer and ground layer within a substrate act as the upper and lower walls and the vias on both sides of the structure act as side walls. This topology makes it possible to implement a nonplanar rectangular waveguide in planar form. The dominant mode in the SIW structure is TE_{10} mode which is similar to the conventional rectangular waveguide. The dispersion constant of the SIW structure can be calculated by the following relation [1-7]:

$$k = 2\pi f \sqrt{\mu_r \varepsilon_{eff}} \quad (2)$$

$$\varepsilon_{eff} = \varepsilon_r \left(1 - \frac{f_0^2}{f^2} \right) \quad (3)$$

Where f is an operating frequency and f_0 is considered as the cutoff frequency of the dominant TE_{10} mode. The μ_r and ε_r represent the permeability and permittivity effect of the substrate that the SIW structure is implemented on it. If $f > f_0$ a positive ε_{eff} and a real k are achieved while if $f < f_0$ a negative ε_{eff} and an imaginary k are obtained. In the second case, it means when $f < f_0$, all field components will decay exponentially away from the source of excitation. Such modes are referred to as evanescent modes. Consequently, when the SIW structure is operated below f_0 , a negative permittivity media can be automatically achieved and k becomes an imaginary number. Therefore, wave propagation is not allowed. From the point of view of the metamaterial concept,

this property is a unique feature of SIW structures. The SIW structure has unique benefits in terms of high power handling capability, low cost, high-quality factor, easy fabrication process and easy integration with other passive components [1-7]. But still, the devices implemented with the SIW structures have large dimensions compared to the microstrip structures. The half-mode SIW (HMSIW) technique, is a miniaturization technique that halves the size of the SIW structures without disrupting the performance and efficiency of the SIW structures [1-7]. The HMSIW structure has been achieved by cutting plane along the magnetic wall and keeps half of the field distribution of the dominant TE_{10} mode.

On the other hand, according to the explanation of the previous section, the CSR unit cell exhibits an ϵ -negative when excited by an axial electric field. Consequently, by a combination of two ϵ -negative materials, an ϵ -positive medium is achieved. An ϵ -negative material is derived with the use of HMSIW structure below its cutoff frequency and another with the use of the CSR unit cell. The configuration of the HMSIW-CSR filter is depicted in Fig. 2. The method of operation of the HMSIW-CSR filter is based on the evanescent-mode technique. According to this approach, a forward passband below the HMSIW cutoff frequency is attained by engraving the CSR unit cell on the metal surface of the HMSIW structure. Fig. 3 shows the simulated frequency responses of the HMSIW-CSR filter. A forward passband below the cutoff frequency of the HMSIW structure has been obtained at $f_r = 2.40$ GHz. Fig. 4, illustrated the real part of ϵ and μ of the designed HMSIW-CSR filter which proves that a positive ϵ achieved at 2.40 GHz. This figure confirms that an ϵ -positive environment can be obtained by merging two environments with ϵ -negative. The simulated unwrapped phase of the HMSIW-CSR filter is shown in Fig. 5. The phase is negative at 2.40 GHz which verifies that the forward propagation below the HMSIW cutoff frequency is occurred. Fig. 6 illustrates the curve of the attenuation constant and the curve of the normalized dispersion relation of the HMSIW-CSR filter. According to the attenuation constant curve, there are two passbands which one of them is the intrinsic HMSIW high passband and another passband is the forward-wave passband below the cutoff frequency of the HMSIW structure which confirms that an additional passband has been achieved. The positive slope of the dispersion curve at 2.40 GHz validates the forward-wave nature of the passband that occurred below the HMSIW cutoff frequency.

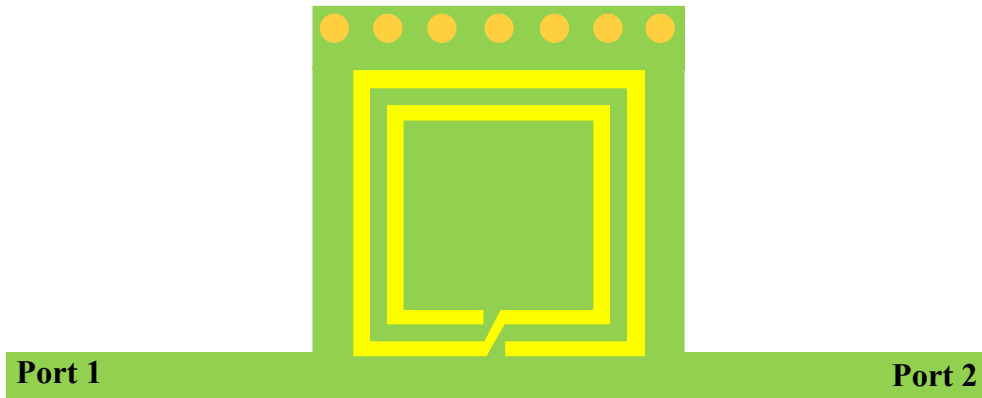


Fig. 2. Configuration of the HMSIW-CSR band-pass filter

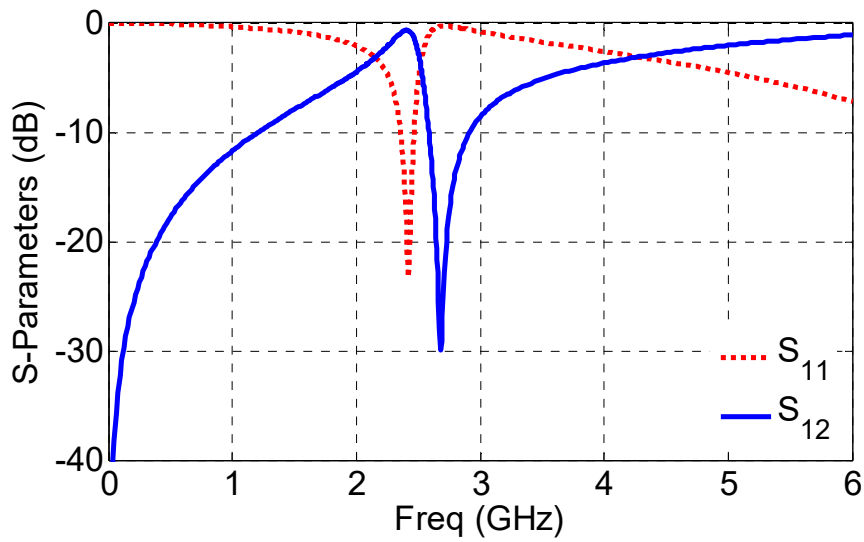


Fig. 3. Simulated frequency responses of the HMSIW-CSR band-pass filter

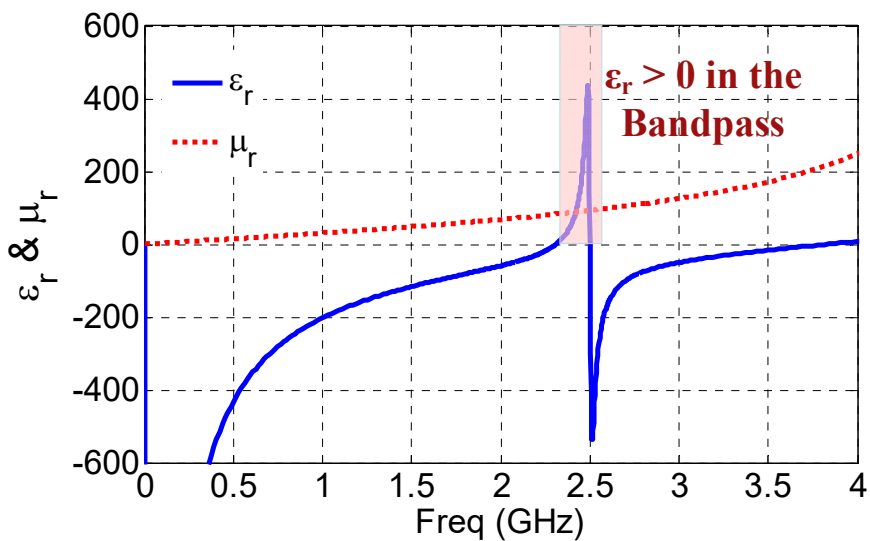


Fig. 4. Extracted real part of the ϵ and μ for the HMSIW-CSR band-pass filter

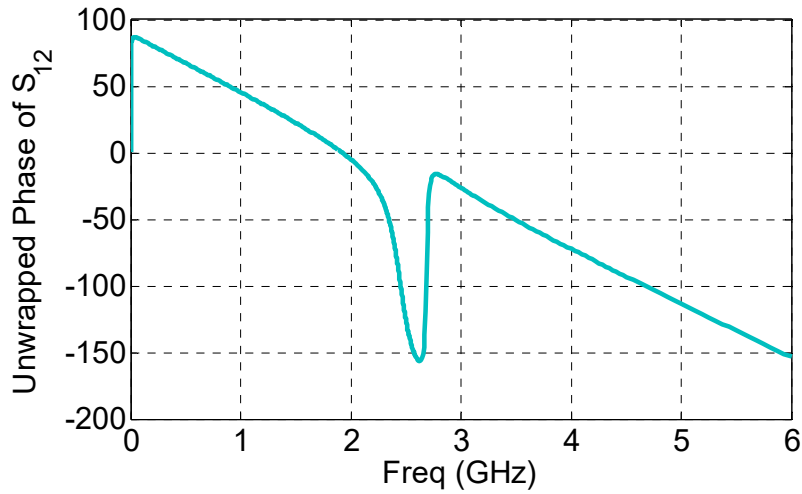


Fig. 5. Simulated unwrapped phase for the HMSIW-CSR band-pass filter

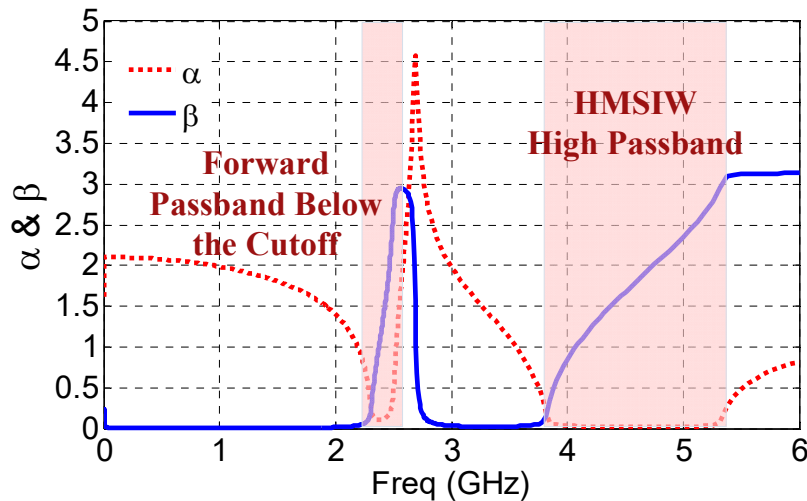


Fig. 6. Dispersion and attenuation diagrams for the HMSIW-CSR band-pass filter

The proposed filtering power dividers (FPDs) with arbitrary power division ratios using the HMSIW-CSR structure are designed and simulated. The recommended equal FPD is shown in Fig. 7. Fig. 8 represented the simulated frequency responses of the proposed equal HMSIW FPD. The whole size of the proposed HMSIW-CSR FPD is about $4.5 \text{ mm} \times 4.1 \text{ mm}$ ($0.067 \lambda_g \times 0.061 \lambda_g$), where λ_g is the guided wavelength in dielectric at the central frequency. The goal of reducing the size of the structure has been achieved by using two techniques which are the half-mode technique and the spiral technique. The filtering properties of the presented power dividers have been obtained using two techniques which are the evanescent mode technique and the spiral technique.

The suggested unequal FPD is also shown in Fig. 9. The simulated frequency responses of the proposed unequal HMSIW-CSR FPDs with the power division ratios of 1:4, and 1:8 are presented in

Fig. 10 (a) and (b), respectively. The different power division ratios could be achieved by changing the locations of the output ports which is plotted in Fig. 11. The power division ratios of the proposed FPDs can be regulated by varying the locations of the output ports. The Fig. 11 confirms that; the power division ratio can be increased simply by increasing the value of w_4 . Moreover, the center frequency of the proposed equal/unequal FPDs can be simply adjusted by resizing the CSR unit cell. The insertion loss (IL) and the bandwidth of the passband can be tuned by changing the values of l_1 and w_3 . The phase difference between the two output ports over the entire operating bandwidth of the proposed equal/unequal HMSIW-CSR FPDs are shown in Fig. 12.

The design steps for implementing the proposed HMSIW-CSR FPDs have been summarized as follows:

1. The cut-off frequency of the dominant TE_{10} mode for the proposed configuration can be tuned by altering the values of w_1 , d , and p .
2. The center frequencies of passband can be adjusted simply by varying the dimension of the CSR unit cell (the values of w_2 , l_2 , s , and c).
3. The bandwidths, insertion losses and return losses of the proposed configuration can be regulated by varying the values of l_1 and w_3 .
4. The power division ratios of the proposed FPDs can be controlled by changing the value w_4 .

The dimensions of the fabricated HMSIW-CSR FPDs are listed as follows: $w_1 = 4.5$ mm, $w_2 = 3.6$ mm, $w_3 = 0.5$ mm, w_4 (“ Δ_{out} ” = 0 dB) = 0 mm, w_4 (“ Δ_{out} ” = 6 dB) = 2.7 mm, w_4 (“ Δ_{out} ” = 9 dB) = 3.3 mm, $l_1 = 0.25$ mm, $l_2 = 3.6$ mm, $l_3 = 4.1$ mm, $s = 0.2$ mm, $c = 0.2$ mm, $d = 0.8$ mm, $p = 1.5$ mm. All of the designed structures are simulated using the ADS electromagnetic simulator. In the equal FPD, the simulated center frequency is located at 2.4 GHz, with a 3 dB bandwidth of 550 MHz ranging from 1.95 to 2.5 GHz which means the fractional band width (FBW) is approximately 23%. Within the passband, the simulated insertion loss is around 0.5 dB, and Δ_{phase} is $<0.04^\circ$. Moreover, the in-band return loss is better than 20 dB. In the unequal power divider with $\Delta_{out} = 6$ dB, the simulated results illustrate the center frequency is located at 2.4 GHz, with a 3 dB bandwidth of 500 MHz ranging from 2 to 2.5 GHz which means the FBW is approximately 21%. Within the passband, the simulated insertion loss is around 0.6 dB, and Δ_{phase} is $<0.03^\circ$. Moreover, the in-band return loss is 27 dB. In the unequal power divider with $\Delta_{out} = 9$ dB, the simulated results illustrate the passband is centered at 2.4 GHz, with a 3 dB bandwidth of 500 MHz ranging from 2.05 to 2.55 GHz which means the FBW is approximately 21%. Within the passband, the simulated insertion loss is around 0.7 dB, and Δ_{phase} is $<0.4^\circ$. Moreover, the in-band return loss is 20 dB.

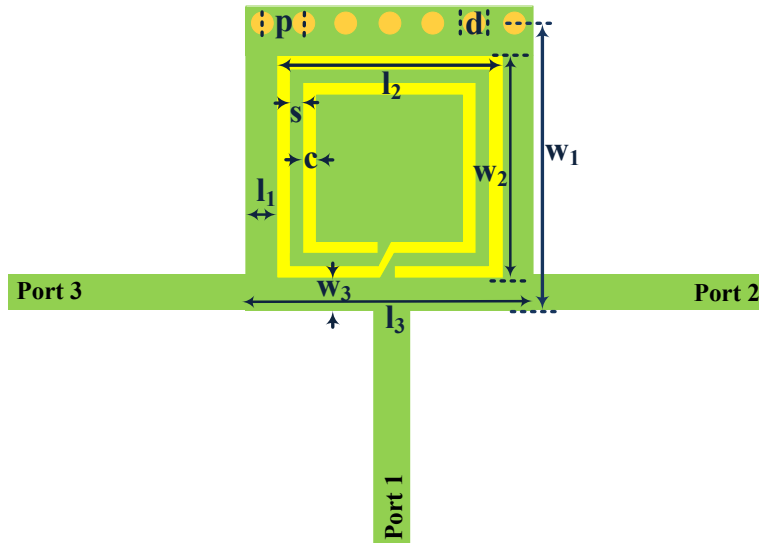


Fig. 7. Configuration of the proposed equal HMSIW-CSR FPD

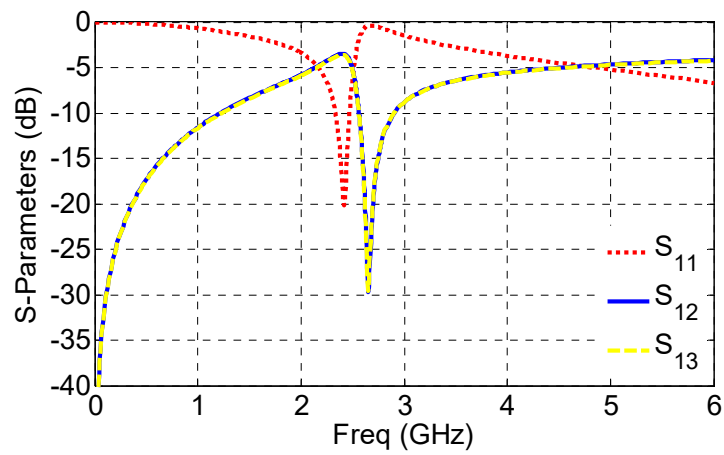


Fig. 8. Simulated results of the proposed equal HMSIW-CSR FPD

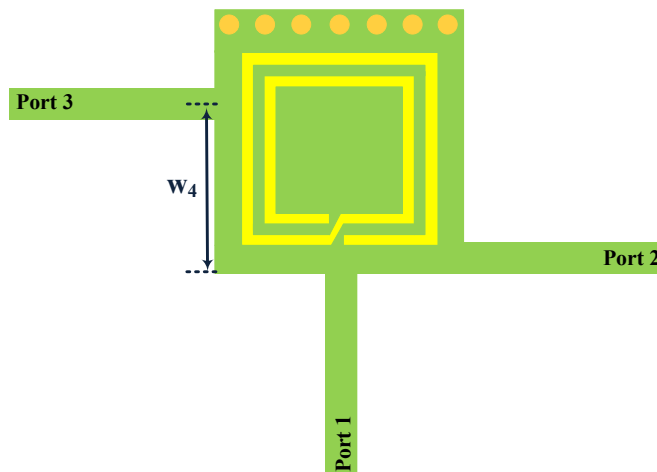


Fig. 9. Configuration of the proposed unequal HMSIW-CSR FPD

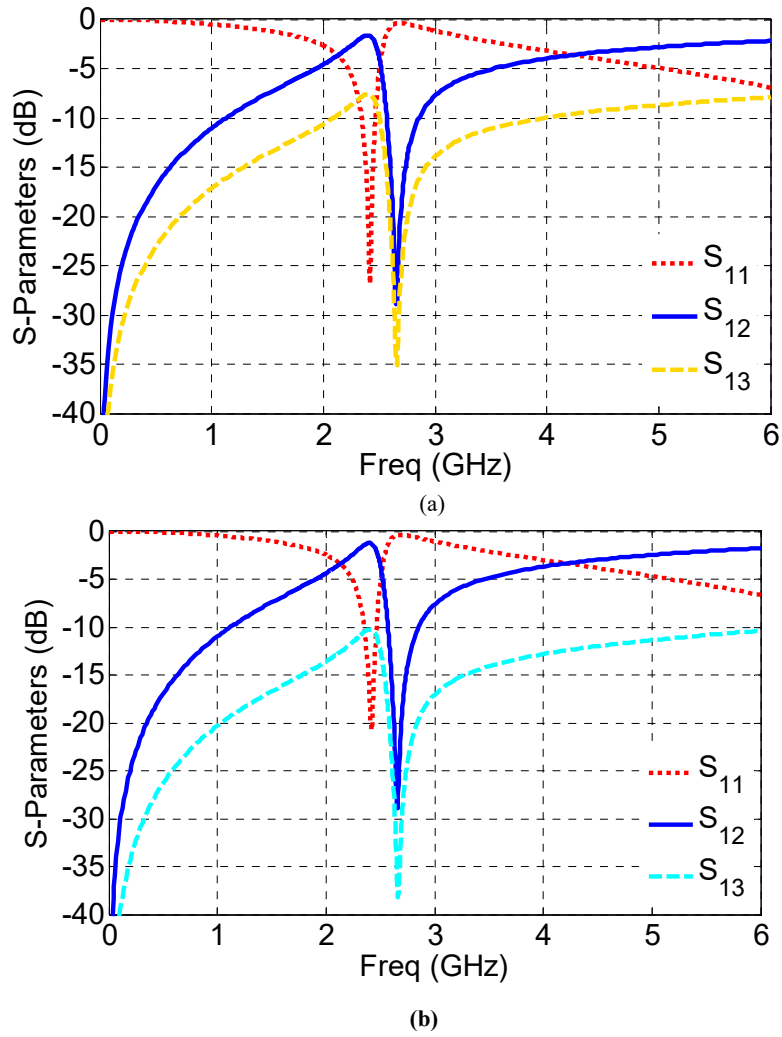


Fig. 10. Simulated results of the unequal HMSIW-CSR FPD (a) “ Δ_{out} ” = 6 dB and, (b) “ Δ_{out} ” = 9 dB

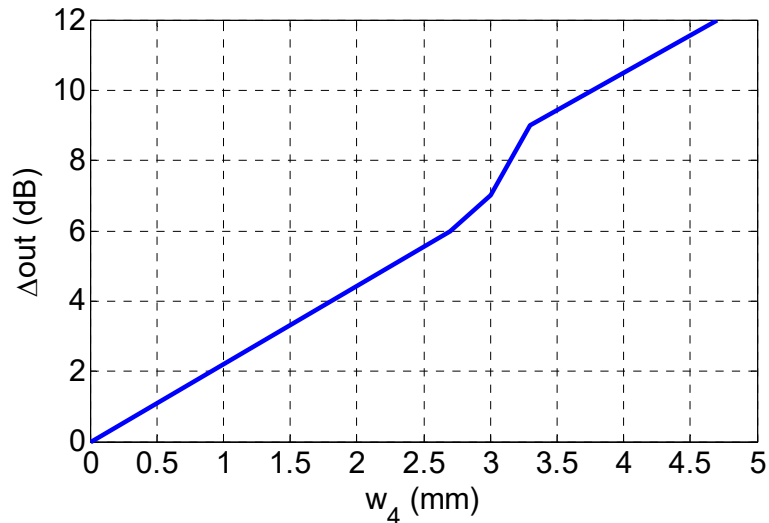
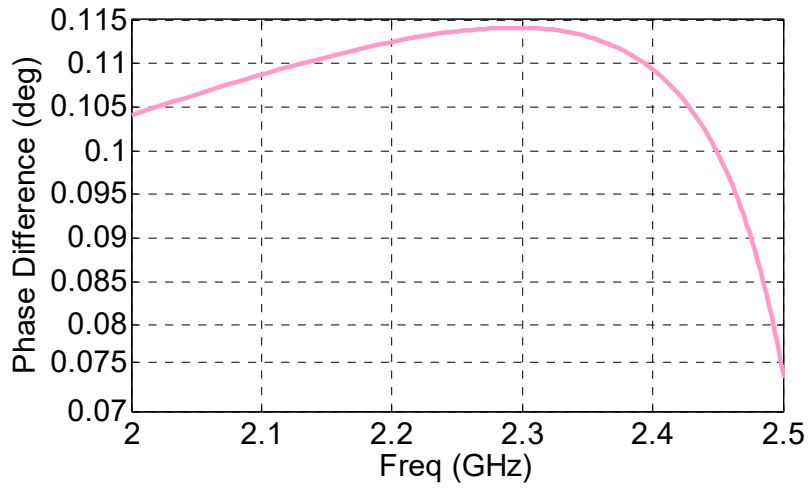
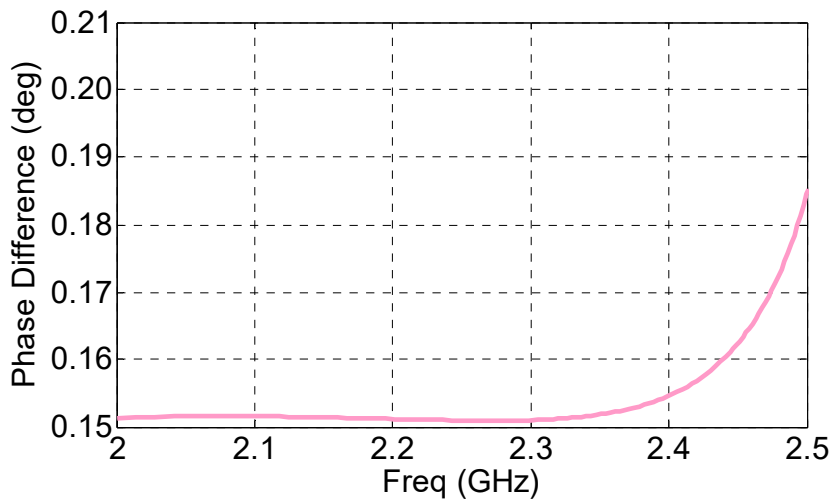


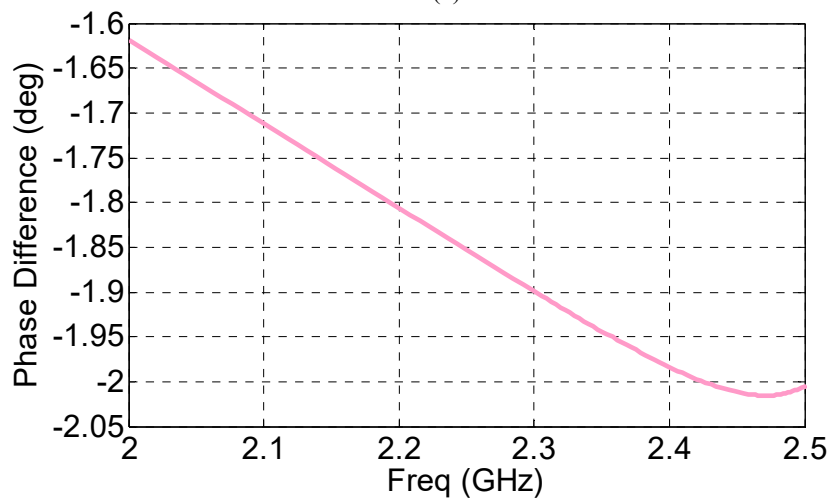
Fig. 11. The “ Δ_{out} ” of the proposed HMSIW-CSR FPDs as a function of w_4



(a)



(b)



(c)

Fig. 12. Simulated differential phases of the proposed equal/unequal HMSIW-CSR FPDs: (a) " Δ_{out} " = 0 dB, (b) " Δ_{out} " = 6 dB, and (c) " Δ_{out} " = 9 dB

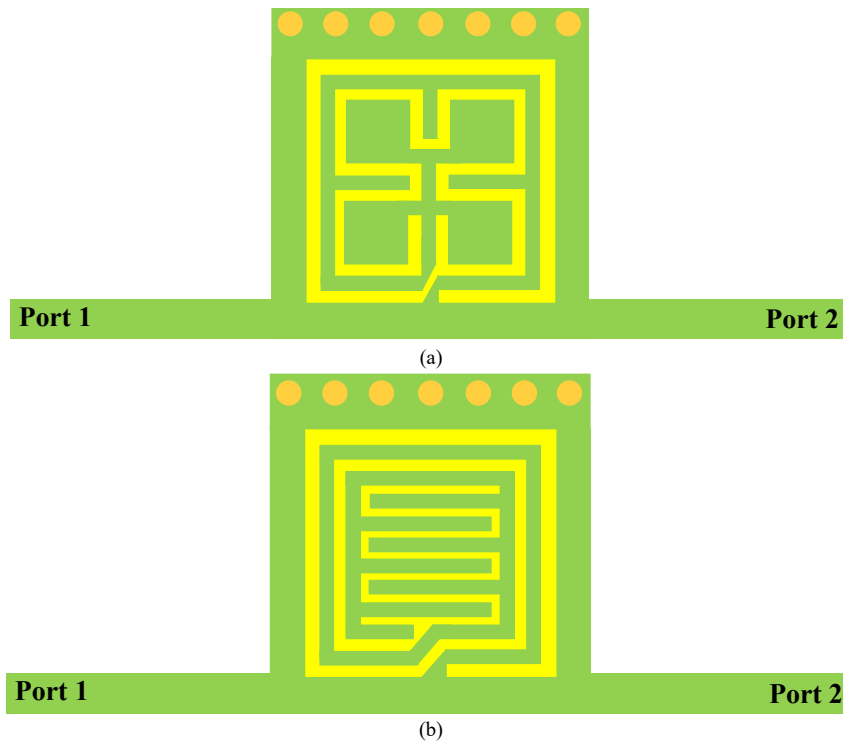


Fig. 13. Configuration of the miniaturized HMSIW-CSR band-pass filters using (a) the fractal complementary spiral resonator (FCSR) unit cell and, (b) the meander complementary spiral resonator (MCSR) unit cell

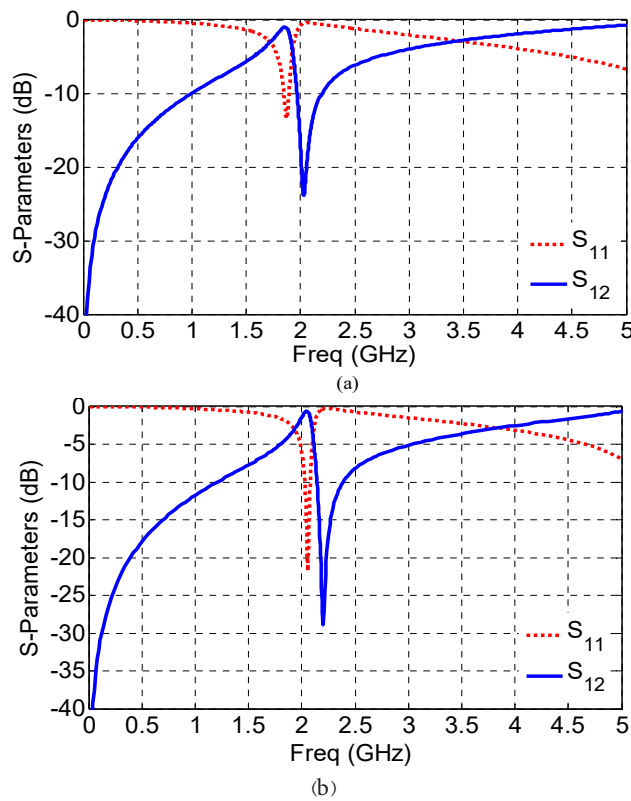


Fig. 14. Simulated frequency responses of the miniaturized HMSIW-CSR band-pass filters using (a) the fractal complementary spiral resonator (FCSR) unit cell and, (b) the meander complementary spiral resonator (MCSR) unit cell

To further reduce the total dimensions, the fractal and meander techniques can be used. Fig. 13 shows the HMSIW bandpass filter loaded by the fractal complementary spiral resonator (FCSR) unit cell, and the meander complementary spiral resonator (MCSR) unit cell, respectively. The resonance frequencies of the FCSR unit cell and the MCSR unit cell, are less than compared to the conventional CSR with the same sizes. Therefore, their electrical sizes are decreased without occupying the extra spaces. That is, by utilizing these unit cells instead of the conventional CSR, the whole physical size of the proposed structure can be reduced without altering its central frequencies. Accordingly, further miniaturization has occurred. The simulated frequency responses of the proposed HMSIW filter loaded by the FCSR unit cell and MCSR unit cell with the same size as the conventional CSR unit cell have been shown in Fig 14. As confirmed in this figure, the resonance frequencies for the FCSR unit cell and the MCSR unit cell have occurred at 1.8 GHz and 2.05 GHz, respectively. Accordingly, by using the fractal and meander techniques, the resonance frequencies become lower compared to the conventional CSR unit cell with identical sizes.

IV. Fabrication and Measurement Results

The photograph of the fabricated FPDs with power division ratios of 1:1, 1:4, and 1:8 is shown in Fig. 15. The Rogers RO4003C substrate has been used to realize the designed equal/unequal FPDs with a thickness of 0.508 mm, dielectric permittivity of 3.55, and loss tangent of 0.0027. All of the designed FPDs are simulated using the ADS electromagnetic simulator. The experimental measurements have been achieved by the employment of a vector network analyzer (VNA) Rohde & Schwarz, zvk through 50 Ω subminiature version A (SMA) connectors which are connected at the end of each port. Reasonable agreements between the measured and simulated results are found. The little difference between the measured and simulated results can be attributed to the tolerance of the dielectric constant, fabrication errors, and the insertion loss of SMA connectors. The proposed equal/unequal HMSIW-CSR FPDs have a total size of 4.5 mm \times 4.1 mm ($0.067 \lambda_g \times 0.061 \lambda_g$). The simulated and measured results for the proposed HMSIW-CSR FPDs are shown in Fig. 16. The recommended equal/unequal HMSIW-CSR FPDs are designed at 2.40 GHz which are appropriate for WLAN applications. For the equal power divider, the measured in-band insertion loss and return loss are 0.7 dB and better than 20 dB, respectively. For the unequal FPD with $\Delta_{out}=6$ dB, the measured in-band insertion loss and return loss are 0.8 dB and better than 23 dB, respectively. For the unequal FPD with $\Delta_{out}=9$ dB, the measured in-band insertion loss and return loss are 0.9 dB and better than 20 dB, respectively. Table 1 compares the performances of the proposed equal FPD with some recently reported FPDs. As well as a comparison between the



**Fig. 15. Photograph of the fabricated equal/unequal HMSIW-CSR FPDs:
(a) “ Δ_{out} ” = 0 dB, (b) “ Δ_{out} ” = 6 dB, and (c) “ Δ_{out} ” = 9 dB**

proposed unequal HMSIW-CSR FPD with $\Delta_{out}=6, 9$ and other FPDs is given in Table 2. In these tables, the advantages in size reduction and low insertion loss is very clear. The total size of the proposed FPDs are approximately 0.04, 0.07, 0.08, 0.004, 0.004, 0.30, and, 0.37 of the whole size of the reported FPDs in [1-7], respectively.

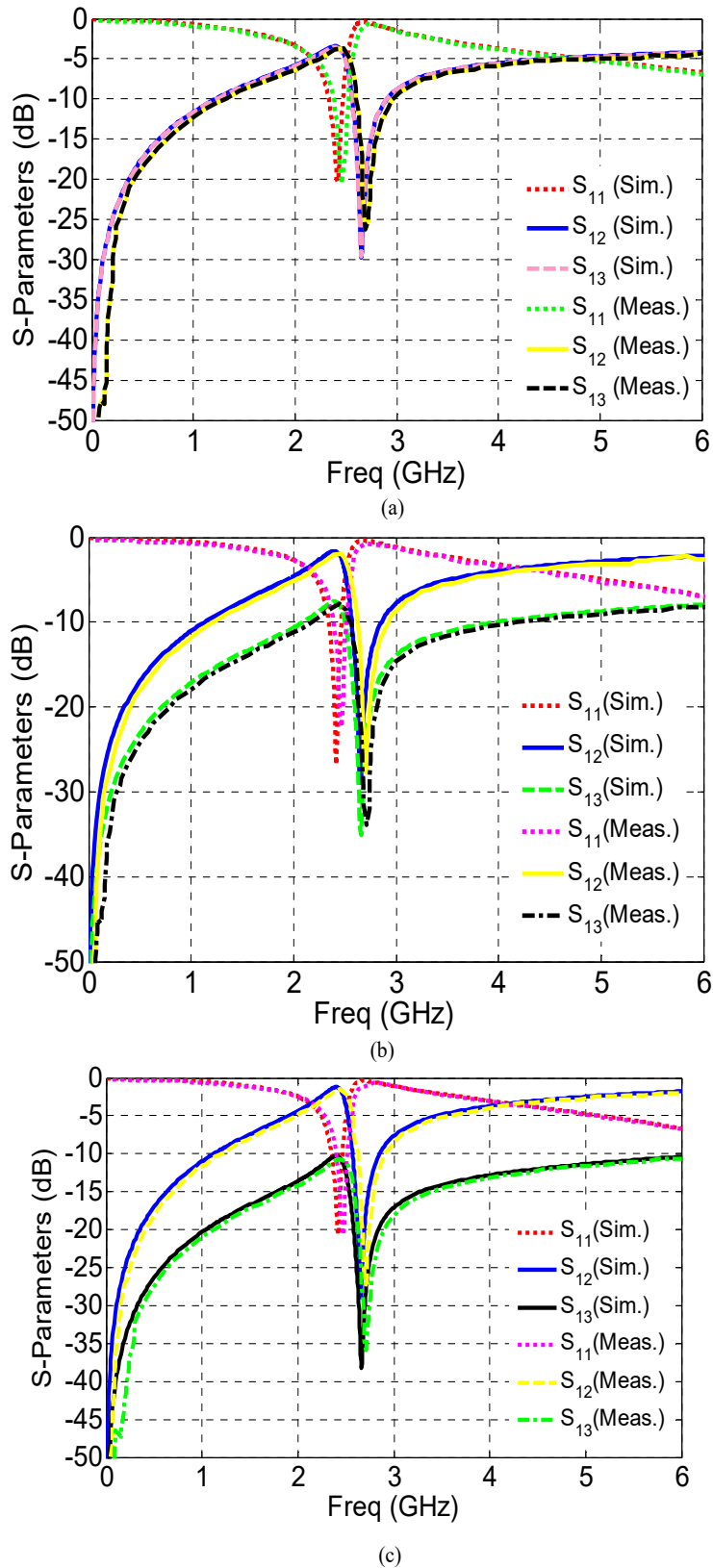


Fig. 16. Measured and simulated results of the fabricated equal/unequal HMSIW-CSR FPDs:
(a) “ Δ_{out} ” = 0 dB, (b) “ Δ_{out} ” = 6 dB, and (c) “ Δ_{out} ” = 9 dB

Table 1. Comparison with other equal FPDs

Ref. Num.	CF (GHz)	IL (dB)	RL (dB)	FBW (%)	Size ($\lambda_g \times \lambda_g$)
[1]	5.82	1.2	24	15.8	0.37×0.21
[2]	5.39	1.3	13	13.73	0.31×0.14
[3]	5.62	1	15	6	0.21×0.18
[4]	3.5	1.3	17	7.75	0.66
[5]	5.61	1.2	14	7.8	0.82×0.81
[6]	2.4	0.5	28	39.5	0.11×0.09
[7]	2.4	0.6	25	21	0.09×0.09
[8]	5.45	1	11	11.2	1.81×0.96
[9]	3.68	1	13	109.7	1.23
[10]	2.45	3.59	15	19.6	0.38×0.25
[11]	1	0.9	16	107	0.36×0.33
[13]	2	3.75	20	70	0.68×0.28
[14]	2	0.7	15	103.56	0.65×0.32
[15]	2.1	0.42	21.4	19	0.45×0.29
[16]	3.26	1.2	15.9	15.9	1.04×0.38
[17]	4	~7	20	75.1	1.25×1.00
Proposed Equal FPD	2.40	0.7	20	23	$0.06 \times 0.06 (=0.003)$

Table 2. Comparison with other unequal FPDs

Ref. Num.	Δ_{out}	CF (GHz)	IL (dB)	RL (dB)	FBW (%)	Size ($\lambda_g \times \lambda_g$)
[1]	6/9	5.73/5.83	1.7/1.3	>20	7.7/11	$0.30 \times 0.16 / 0.30 \times 0.15$
[2]	6/9	5.47/5.68	1.4/1.6	26/17	8.41/8.97	$0.25 \times 0.17 / 0.25 \times 0.18$
[6]	6/9	2.4/2.4	0.4/0.5	27/22	40/38.3	0.11×0.09
[7]	6/9	2.4/2.4	0.6/0.6	18/16	18/18	0.09×0.09
[12]	6/9	2.4/2.4	1.85/1.96	11/11.8	90/100	$0.1 \times 0.6 / 1.28 \times 0.66$
Proposed Unequal FPD	6/9	2.4/2.4	0.8/0.9	22/20	21/21	$0.06 \times 0.06 / 0.06 \times 0.06 (=0.003)$

V. Conclusion

In this paper, three ultra-compact equal/ unequal HMSIW power divider with filtering response is recommended. The whole dimension of the proposed equal/unequal FPDs is only $0.06 \lambda_g \times 0.06 \lambda_g$. By varying the locations of the output ports, the power division ratio can be easily tuned. The 3-dB FBW is approximately 21% from 2 to 2.5 GHz. The phase imbalances

between the output ports of the proposed equal/ unequal FPDs are lower than 0.4° . Three filtering HMSIW PDs with different power division ratios of 1:1, 1:4 and 1:8 are designed and tested to confirm the efficiency of the design method. The simulation and measurement results show an acceptable agreement. The measured results prove the ability of the proposed FPDs in terms of size reduction, easy integration with other planar microwave circuits, low loss, low fabrication cost and high selectivity. Therefore, the proposed equal/unequal HMSIW-CSR FPDs are a good candidate for the implementation of the FPDs with compact size, easy center frequency tunability and arbitrary power division ratio.

References

- [1] M. Danaeian, A. R. Moznebi, K. Afrooz, and H. Hakimi, "Miniaturised equal/unequal SIW power divider with bandpass response loaded by CSRRs," *Electronics Letters*, vol. 52, no. 22, pp. 1864-1866, Oct. 2016.
- [2] M. Danaeian, A.-R. Moznebi, K. Afrooz, and A. Hakimi, "Miniaturized filtering SIW power divider with arbitrary power-dividing ratio loaded by open complementary split-ring resonators," *International Journal of Microwave and Wireless Technologies*, vol. 9, pp. 1827-1832, July 2017.
- [3] A. R. Moznebi, M. Danaeian, E. Zarezadeh, and K. Afrooz, "Ultracompact two-way and four-way SIW/HMSIW power dividers loaded by complementary split-ring resonators," *International Journal of RF and Microwave Computer-Aided Engineering*, vol. 29, p. e21878, Oct. 2019.
- [4] A.-R. Moznebi, K. Afrooz, M. Danaeian, and P. Mousavi, "Four-way filtering power divider using SIW and eighth-mode SIW cavities with ultrawide out-of-band rejection," *IEEE Microwave and Wireless Components Letters*, vol. 29, no. 10, pp. 586-588, 2019.
- [5] A. R. Moznebi, K. Afrooz, M. Danaeian, and P. Mousavi, "Compact filtering power divider based on corrugated third-mode circular SIW cavities," *Microwave and Optical Technology Letters*, vol. 62, no. 5, pp. 1900-1905, May 2020.
- [6] M. Danaeian, "Novel Miniaturized Equal/Unequal HMSIW Filtering Power Dividers Based on the Evanescent Mode Technique," *Radioengineering*, vol. 30, no. 1, pp. 117-124, April 2021.
- [7] M. Danaeian and H. Ghayoumi-Zadeh, "Equal/unequal half mode substrate integrated waveguide filtering power dividers using an ultra-compact metamaterial unit-cell," *Frequenz*, vol. 76, pp. 593-604, April 2022.
- [8] A. R. Moznebi, K. Afrooz, and M. Danaeian, "High performance filtering power divider based on air-filled substrate integrated waveguide technology," *ETRI Journal*, vol. 45, pp. 338-345, 2023.
- [9] A.-R. Moznebi, K. Afrooz, and A. Arsanjani, "Broadband bandpass filter and filtering power divider with enhanced slow-wave effect, compact size, and wide stopband based on butterfly-shaped spoof SPPs," *AEU-International Journal of Electronics and Communications*, vol. 145, p. 154084, Feb. 2022.
- [10] H. Tian and Y. Dong, "Packaged filtering power divider with high selectivity, extended stopband and wideband isolation," *IEEE Trans. Circuits and Systems II: Express Briefs*, vol. 70, pp. 1311-1315, 2022.
- [11] Y. Liu, S. Sun, and L. Zhu, "2 n-way wideband filtering power dividers with good isolation enhanced by a modified isolation network," *IEEE Trans. Microwave Theory and Techniques*, vol. 70, pp. 3177-3187, 2022.
- [12] D. Wang, X. Guo, and W. Wu, "Wideband unequal power divider with enhanced power dividing ratio, fully matching bandwidth, and filtering performance," *IEEE Trans. Microwave Theory and Techniques*, vol. 70, pp. 3200-3212, 2022.

- [13] F. Huang, L. Zhu, X. Hu, J. Zhou, F. Wang, S. Wang, *et al.*, “A Fully Packaged Wideband Bandpass Power Divider Based on Four-Port Common-Mode Network,” *IEEE Trans. Circuits and Systems II: Express Briefs*, 2023.
- [14] L. Liu, K. Chen, Z. B. Wang, and Y. R. Zhang, “Wideband and compact filtering power divider based on vertically installed planar structures,” *International Journal of RF and Microwave Computer-Aided Engineering*, vol. 32, p. e23251, 2022.
- [15] A. Sheikhi and P. Rostami, “Design of a filtering power divider with high selectivity based on coupled lines,” *Microwave and Optical Technology Letters*, vol. 64, pp. 269-275, 2022.
- [16] W.-S. Liu, L. Xu, F. Wei, T. Feng, X.-B. Zhao, Y.-C. Xue, *et al.*, “Miniaturized Single-Ended-to-Balanced Filtering Power Divider with High Selectivity Based on Tri-Mode Resonator,” *IEEE Trans. Circuits and Systems II: Express Briefs*, 2023.
- [17] D. Wang, W. Wang, Q. Tan, H. Yang, Y. Cao, W. Tang, *et al.*, “Design of a four-way out-of-phase wideband filtering power divider with high selectivity response,” *International Journal of RF and Microwave Computer Aided Engineering*, vol. 32, p. e23520, 2022.
- [18] J. D. Baena, R. Marqués, F. Medina, and J. Martel, “Artificial magnetic metamaterial design by using spiral resonators,” *Physical review B*, vol. 69, p. 014402, 2004.

